Pattern Recognition Imaging for AFM Measurements

Mario D'Acunto and Ovidio Salvetti

Instituto di Scienze e Tecnologia dell'Informazione, ISTI-CNR
via Moruzzi 1, I-56124, Pisa, Italy

Abstract. The focus of this paper is on an algorithm for distortion corrections for atomic force microscope (AFM) recorded images. AFM is a fundamental tool for the investigation of a wide range of mechanical properties due to the contact interaction between the AFM tip and the sample surface. When a sequence to AFM images correspondent to the same area are recorded, it is common to observe convolution of thermal drift with surface modifications due to the AFM tip stresses. The surface modifications are material properties and add knowledge to the response of the materials on nanoscale. As a consequence, a suitable de-convolution of the thermal drifts on the recorded images need to be developed. In this paper, we present a method for correcting thermal drifts where the original images are corrected using a low-order polynomial mapping function. The precision achieved and the fast computation time required make our method particularly useful for image analysis in a wide range of applications.

1 Introduction

In the last two decades atomic force microscope (AFM) has been developed well beyond the topographic imaging tool. It has become an important instrument for manipulation and material property characterizations at the nanometer scale. The precision of positioning has always been the key driver for AFM technology and scanning probe microscopy in general. In an imaging tool the uncontrolled hardware drift, such as piezo creep and thermal drift, usually causes image distortion. Some solutions based have been proposed [1-2]. The focus of this paper is to build a method for correcting the thermal drifts that represent the most important source for distortions on sequential recorded AFM images on the same localized area. The recorded data are divided in two classes, one is connected to topographic data, and the second one to elastic surface Young moduli. Such two channel AFM data give the possibility to manipulate data crossing by one class (topography) to the other one (surface elastic map). In special way, the method for image analysis based on drift compensation is particularly useful for time AFM sequential measurements. This last technique is used for studying the response of viscoelastic materials to AFM tip stress. The sample used was a low molecular weight tri-block polycaprolactone-polyethilene glycol-polycaprolactone (PCL-PEG-PCL) copolymers. Tri-block PCL-PEG-PCL copolymers present generally hard islands surrounded by soft materials. Under the stress of an AFM tip, it has been observed that soft polymer materials can cover the hard isl-

D'Acunto M. and Salvetti O. (2010).
Pattern Recognition Imaging for AFM Measurements.
In *Proceedings of the Third International Workshop on Image Mining Theory and Applications*, pages 68-77
DOI: 10.5220/0002962600680077

ands. This wearing phenomenon for viscoelastic materials does not have a clear and exhaustive explanation due to the difficult to quantify the soft polymer coating the hard islands. Making use of the image analysis based on drift compensation it is possible to reduce the drift in sequential AFM measurements and calculate with accuracy the soft polymer volume moved by AFM tip. Our method is divided in two steps. In the first one, we identify using a cross correlation function the residual thermal drift. In the second step, we introduce a function connected to the thermal drift and a set of specific parameter connected to low-order polynomial mapping function. The minimization of such mapping function leads to the optimal parameters removing the drifts from the sequence of the AFM images of viscoelastic sample using an useful pattern recognition matching the images correspondent to same sample areas recorded in different times. Our proposed method should become a powerful tool for the accurate analysis of stressed viscoelastic surface and accurate quantification of AFM multichannel measurements.

2 Numerical Methods for Image-based Adaptive Drift Compensation

The possibility of investigation of surface properties of viscoelastic materials using AFM is based essentially on a sequence of scans on the same area to be observed. The interpretation of data is complicated by two main factors: *i*), the presence of drifts does difficult to compare AFM images acquired in different times on the same sample location; *ii*), the accurate identification of specific morphological deformations of viscoelastic materials due to stressing tip resulting in a modified sequential images with respect to the first primitive image, so leading to misinterpreted data. Since AFM generates multiple image channels simultaneously, the spatial and temporal correlation of patterns in these channels can substantially enhance the robustness of the pattern detection and its position measurement, see appendix. Furthermore, the raster scanning of a probe across the same pattern back and forth embeds asymmetric feedback control signatures for widely contact mode imaging. These signatures provide a powerful tool to distinguish a true pattern from a set of noisy data. Reliable pattern positioning data enable a precise adaptive control which should achieve a sub-nanometer positioning accuracy over long period of time. The forward scan (trace) and the reverse scan (retrace) of the same location also provide independent information of the same patter location. In this paper, we will consider two channels correspondent to the topographic data (first channel, quantitative data) and surface elastic Young moduli data (second one) measured using the modulation force AFM tool. The topographic data correspond to the height $z=f(x,y)$ measured by the AFM tip scanning the sample surface, see figure 5 (left). On contrary, the modulation force channel measures in a qualitatively way the differences of surface elasticity. Modulation force is a powerful tool for the knowledge of surface properties, nevertheless when the AFM is used for a time sequence scanning cycle on the same viscoelastic sample area, it is strongly limited by its qualitatively nature.

We adopt a new method integrating a numerical corrections of thermal drifts with pattern recognition imaging. A cross correlation function is used a priori as a method

for the definition of the possible range of thermal drift to be identified. There are mainly two approaches to connect pattern recognition with location of specific features on multi-channel images: template based method or parametric one. Template based algorithms locate regions on the image that matche a known reference pattern. They bare applicable when well defined and slowly changing patterns are available on the image. Multi-channel AFM images can improve pattern location accuracy by matching all the channels of images with their own templates, while these templates are spatially correlated, figg. 1-2. Parametric based algorithms can be applied when focused patterns are changing from image to image and cannot be described by image template. These patterns, however, can be indentified by a set of measurable variables such as geometrical and regression properties that are restricted to a certain parameterized region in the space of measured variables. Parametric algorithms based on geometrical patterns and spatial correlation of combined AFM images have been developed to locate the surface pattern with sub-pixel resolution in real time [2]. It is commonly recognized that a robust and precise drift measurement tool based on imaging patterns is needed in order to compensate thermal drift without causing positioning errors. Kalman filter provides the best results when dynamics of the system is accurate and noise statistical parameters are fixed and known a priori. Unfortunately, this is not generally the case for AFM measurements where both dynamics and noise statistics may change in time and depend on viscoelastic sample, tip and environment (humidity, temperature, etc.). In this situation, with inaccurate model and/or underestimated statistical parameters of the noise, Kalman filter may diverge, i.e., its estimation has errors that are much greater than predicted by theory [2]. The general challenge in image analysis of AFM measurements is to provide accurate and reliable tools to precisely locate the imaging pattern and implement real time control according to specific applications requirements.

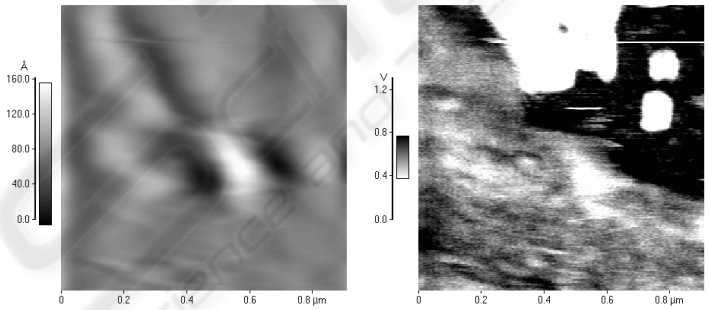

Fig. 1. A two channels AFM image of the tri-block PCL-PEG-PCL copolymer. On the contrary to topographic data (left), the FMM image (right) shows characteristic hard domain (brighter) surrounded by softer matrix (dark). The hard domains are approximately cylinders with the principal axe normal to the surface. The zoom of the area surrounding the hard islands in the Modulation force mode image are reported in the figure 2. The area considered was 1µm×1µm.

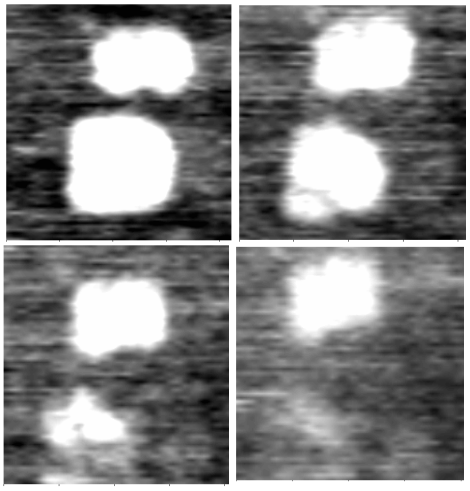

Fig. 2. Modulation Force (FMM) recorded data of 200nm×200nm areas showing two hard PU islands (bright regions) surrounded by soft matrix (darker areas). From A-to-D: progressive reduction of the stiff areas (white-to-grey) induced by the repeated passage of the AFM probe tip.

2.1 A New Method for the Correction of AFM Drifts

The correction of drifts on viscoelastic AFM images is complicated by the overlapping of surface effects due to tip stress that can drag polymer material from a site to another one. As a consequence, if the displacement due to the drift, $\Delta\mathbf{r}$, is known during the scanning of an image, it should be possible to apply a correction based on $\Delta\mathbf{r}(t)$ to the scanned image to recover an undistorted image. The correction can be expressed as a mapping $(x,y)\rightarrow(x',y')$ between the set of points (x, y) in the image and a new set of coordinates (x',y'), based on the time each point was scanned. Generally, the z-direction, i.e., the height would be not affected by relevant drifts, in special way thermal drifts. This implies the brightness of any pixel can be considered as the "true" value of the measurements. An other important feature of distortions is due to the slow scanning axis. Generally, the slow scanning axis is the y-axis, while the fast scanning axis is the x-axis. We can rewrite our mapping function $(x,y)\rightarrow(x',y')$ as [3]:

$$x' = x + \Delta r_x(y) \qquad y' = y + \Delta r_y(y) \tag{1}$$

Thermal changes is the main source for drifts on AFM image on viscoelastic materials, other distortions could arise by deformation of scanning tip or nonlinearity in the xy stage or non-orthogonality between the x and y and z axes, can lead to positional errors that are functions of x and z. In our measurements, the incidence of such distortion are not present, so we limit ourselves essentially to thermal drift. If thermal drift is the main source drift, then changes of relative positions are not expected. If

the slow scanning is the y-axis, each horizontal can line may be shifted either up, down, right, or left with respect to its neighbors, the scan line itself remains intact and unchanged. This is because we only need to rescan a small vertical portion of the original image and the displacement of each scan line at its center can be used as a correction for the entire scan line.

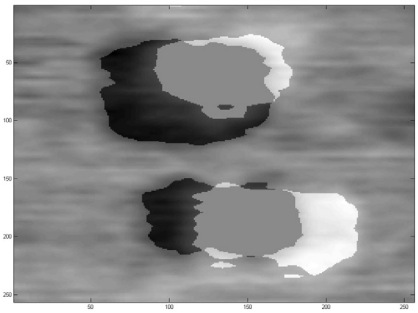

Fig. 3. Overlapping of the first and the 30-th image recorded on the same location of the viscoelastic sample before treatment. The shift of the hard domains could be due to thermal drift or specific viscoelastic features due to tip stressing. Our computational methods should be able to discriminate between the two sources of shifting. The alignments were made using a cross correlation function, eq. (3).

Because thermal drift is a slowly varying, smooth function, we can model it as a low order polynomial along y-direction. For moderate drift a suitable third order polynomial could work:

$$x' = x + A_0 + A_1 y + A_2 y^2 + A_3 y^3$$
$$y' = y + B_0 + B_1 y + B_2 y^2 + B_3 y^3 \quad (2)$$

Mathematically our target is the solution of the system equations (2), i.e., to find the set of parameters $[A_0, A_1, ..., B_3]$ which, when applied to both the original scan yields the minimum difference between the overlapping areas of two corrected images, as in figure 3. This problem is a main topics of the broad subject of image registration, an active area of research in computer science and numerical programming [3-5]. In comparing two images, there are two broad strategies one could pursue: i) comparing the two images pixel by pixel; or, ii), comparing specific lists of features that have been identified in each of the images. The first strategy has the significant disadvantage that there are many more pixels than identifiable features, leading to algorithms that are computationally intensive and in some sense inefficient.

The alternative strategy requires some method for identifying the appropriate features in the images, and this raises too many problematic issues for a method to be applicable to any scanned image. In addition some surface effect due to stressing tip on the viscoelastic sample can produce misunderstanding features using such strategy.

Following Salmons et al. [3], we adopt a strategy based on pixel-to-pixel approach introducing a minimum difference function, defined as the minimum root-mean-

square (*rms*) difference between the pixel value of the sequence of corrected images and the sequence of original images. The sequence of corrected images is found applying a cross correlation function. The cross correlation function for two arrays A and B of discrete data points is given by [6]:

$$\Gamma\left(\Delta x, \Delta y\right) = C.\sum_{j=1}^{N_j}\sum_{i=1}^{N_i} A\left(i, j\right).B\left(i+\Delta x, j+\Delta y\right) \tag{3}$$

where N_i (N_j) is the number of data per row (column) and C is a normalization constant. The position (Δx,Δy) of the maximum of the cross correlation function gives the lateral shift of the images relative to each other. If the shapes of the two surfaces are identical, the maximum lies at (0,0). To prevent the indices in the above formula from running out of range, the performance of the cross correlation has to be restricted to a smaller area inside the actual images leaving a border of the least the same size as the expected image shift. Once the corrected images have been found with a cross correlation function, eq. (3), we can minimize the set of parameters [A_0, A_1,...B_3], introducing the *diff-function* defined as [3]:

$$diff-function\left[A_0, A_1, ..., B_3\right] = \sqrt{\sum_{j=1}^{N_j}\sum_{i=1}^{N_i}\left[z_t\left(i, j\right) - z_s\left(i, j\right)\right]^2} \tag{4}$$

where z is the pixel value of an image at a particular point (i,j), z_t and z_s are the corrected data image and the source (as recorded) data image, respectively. Eq. (4) means that the mapping function (x,y)→(x',y') to an area of the main image extending beyond its own center, maximizing the area available for comparison between the two corrected images. We have to find a global minimum of this function over the allowed parameter space; in fact, there may be many local minima. A robust method is based on using a grid search, where to evaluate the diff-function for all possible values of all eight parameters (that is, for all points an eight dimensional grid). Nevertheless, such method is too slow to be used on a sequence of images. In this paper we present an alternative strategy based on an preview estimation of the most probable couple (Δ_x,Δ_y) found as the maximum of the cross correlation function. Because the shift is expected in the direction of the x-direction, figure (4), we can select a strip divided in different block numbered by δ. A this point the diff-function can be limited to three only parameters:

$$diff-function\left[\delta, \Delta x, \Delta y\right] = \sqrt{\sum_{j=1}^{\delta_{N}j}\sum_{i=1}^{\delta_{Ni}}\left[z_t\left(i+\Delta x, j+\Delta y\right) - z_s\left(i, j\right)\right]^2} \tag{5}$$

with the precalculation made with cross correlation function, evaluating the difference function for each new set of parameters now consists of looking-up and summing a series of array values in *diff-function*[δ, Δx, Δy], one for any block δ. To minimize the overhead of this reevaluation, parameters lists are carefully sorted, so that all possible parameter sets for each range of (Δx,Δy) are exhausted before reevaluating *diff-function*[δ, Δx, Δy].

The incidence of the thermal drift is the same on both the channel AFM data, topography and surface elastic moduli. We have operates the correction drift on

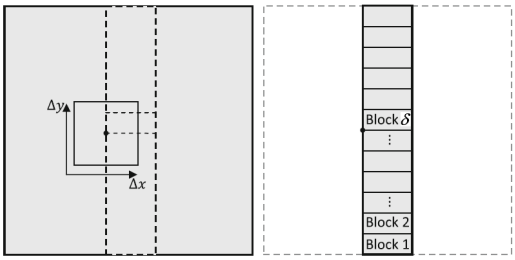

Fig. 4. Scheme showing the identification of a possible shift described by a couple (Δx,Δy) identified with a cross correlation function. On right the stripe containing the possible shift due to thermal drift along the slow scanning direction.

the modulation force data, but we can use such information on the topographic data where pattern recognition was rather hard to do. As a consequence, after undergoing the adjustment procedure, the new surface images correspondent to the corrected topographic data, denoted by A^* and B^*, can be compared quantitatively. We quantified the amount of volume change between the subsequent recorded data. This has been done by integrating over the difference of the image data correspondent to the recognized area:

$$\Delta V = \sum_{\substack{j=1 \\ i=1}}^{N_j^*, N_i^*} \left[B^*(i,j) - A^*(i,j) \right] \tag{6}$$

3 Results and Discussion

The algorithm for the correction of the drift in the AFM imaging sequence was carried out in two steps. In the first step, the images had to be laterally adjusted using the cross correlation function, eq. (3). The couple (Δx,Δy) that maximizes the cross correlation function was found [4]. In the second step, we applied the *diff-function* restricted to three parameters [3] to the sequence of recorded images. The application of these two steps was justified by the fact that all the observed image shifts showed translation movement and a small degree of rotation, figure 3, [6]. After undergoing the adjustment procedures, the new surface images were compared quantitatively, figures 5 and 6, and the degree of change in wear volume was calculated, figure 7.

The restricted *diff-function* demonstrated to be an efficient and robust algorithm for the minimization finding with respect to grid search. To have an idea how the computation scales, suppose that the maximum amount of the distortion drift remains constant ad a fraction of the image height (say, 5%), but that the number of pixels N in the image is doubled. Maintaining single-pixel precision in the grid search requires that the number of values of each of the parameters [A_0,A_1,...,B_3] also be doubled. For each set of parameters, the number of blocks in y-direction to be evaluated would also be doubled. Thus for a third order polynomial fit, the grid search should scales as $O(N^9)$. Practically, downsampling an image by a factor of two should cut the time of

the grid search by more than a factor of 100. Subdividing an image in two and correcting each half independently would have a similar impact on computation time, but would make the method less robust to image artifacts. To have an estimation of the computation time achieved by our method, we timed our program on a single 256×256 pixel image, running it on a desktop computer with a single Intel Core I7 processor running a 2.93GHz. The search for the couple (Δx,Δy) using the cross correlation function and then the minimization of the *diff-function* [δ, Δx, Δy] on the sequence of 30 images required approximately 22 s.

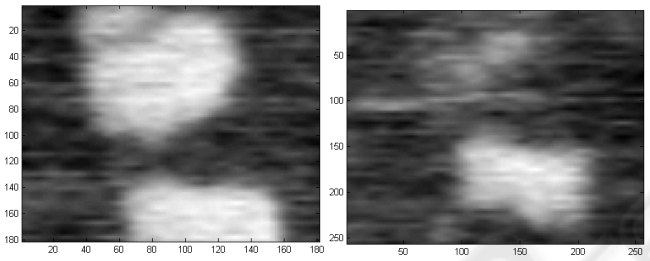

Fig. 5. Comparison between the first and 30-th scan after the correction of thermal drift. The thermal drift is quantified by *diff-function* minimization as approximately 10nm, i.e., 5% of the entire scanning length.

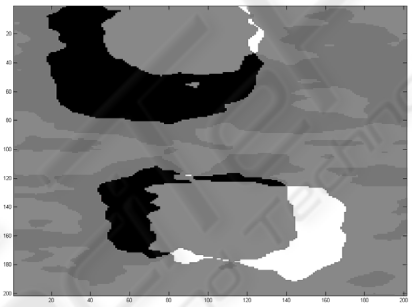

Fig. 6. This image is the equivalent of figure 3 after the correction of thermal drift using our procedure algorithm. The overlapping of the first and the 30-th image recorded on the same location of the viscoelastic sample present now a region of the hard island that has been coated by the polymer. Analogously, a shift independent by thermal source is present indicating that the hard island moved by the initial location due to reorganization of the polymer soft matrix. If our results are confirmed by further studies and refinements of our algorithms, new insights on the nanoscale dynamics of soft surface could be identified.

An important parameter that describes the tri-block copolymer sample surface modifications induced by the AFM tip is the volume change between subsequent images [5]. The volume can be calculated by integrating over the difference following the expression (6) using two subsequent acquired AFM images after adjustment. The volume evaluation is performed on the topographic images once the drift are corrected on the modulation force. The behaviour of the volume changes between subsequent images is shown in figure 7.

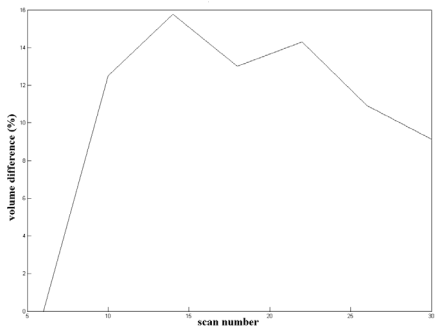

Fig. 7. Volume changes as calculated using eq. (2) between subsequent images. The volume is calculated on topographic data correspondent to the re-aligned and computationally corrected FMM images.

The volume variation between subsequent images presents a fast growth after an activation barrier is reached. During the first scans the soft polymer component presents a resistance to tip induced stress. When the stress drops the activation, then the volume percentage approaches to a sort of plateau with reduced fluctuations. It is interesting as shoed by figure 6, that the hard islands shift position making so more difficult for the soft component to coat the hard regions. All such results can be well interpreted only after computational manipulation as above described. Many problem are still open and they can be well known only after many dedicated experiments and suitable computational algorithms. Our computational image analysis results seem go in this direction.

4 Conclusions

The investigation of viscoelastic materials using AFM instrumentation is particularly powerful to define the surface properties on molecular and supramolecular scale. When a repeated sequence of AFM images on the same area, the images present a convolution of thermal drifts and material-related modified features due to AFM tip stressing. In this paper, we develop some algorithms for the accurate deconvolution of thermal drift from the specific surface viscoelastic modifications. Our method corrects the thermal drift using a low-order polynomial mapping function. The method is robust and requires short computation time, making suitable its shearing on a wide range of applications where image analysis is required.

References

1. Yurov, V. Yu., Klimov, A. N.,: Scanning tunneling microscope calibration and reconstruction of real image: Drift and slope elimination. Rev. Sci. Instrum., 65 (1994) 1551-7
2. Clayton, G. M., Devasia, S.,: Image-based compensation of dynamic effects in scanning tunneling microscopes. Nanotechnology 16 (2005) 809–818

3. Salmons, B. S., Katz, D. R., Trawick, M.L.,: Correction of distortion due to thermal drift in scanning probe microscopy. Ultramicroscopy, available on line.
4. Gonzalez, R., Wood, R.,: Digital Image Processing. Upper Saddle River, NJ, Prentice Hall (2008).
5. Colantonio, S., Gurevich, I. B., Salvetti, O.,: A two-step approach for automatic microscopic image segmentation using fuzzy clustering and neural discrimination. Pattern Recognition and Image Analysis, 17 (2007) 428 - 437.
6. Lazzeri, L., Cascone, M.G., Narducci, P., Vitiello, N., D'Acunto, M., Giusti, P.,: Atomic force microscopic wear characterization of biomedical polymer coatings. Tribotest, 12 (2006) 257-265.

Appendix: Background on AFM and Modulation Force Analysis

The technique for wear testing consisted in using the AFM probing tip to abrade the surface of PU sample for approximately 30 scans while simultaneously imaging the area where the polymer was being progressively damaged by the scanning tip.

The measurements were carried out making use of an Autoprobe CP AFM (Park Scientific Instruments, Sunnyvale, CA) operating in contact mode. The measurements were performed in air at room temperature and relative humidity, nearly 40%. Images of different areas (256pixels×256 pixels) were acquired using silicon tip (conical shape, nominal probe radius of 10nm, nominal cantilever stiffness 0.24N/m, from PSI manufacturer). Topographic images of square areas of 200nm×200nm were acquired with silicon microlevers with a spring constant of $0.24 Nm^{-1}$, and nominal radius of 10nm. In addition to topography, mechanical properties qualitative information has been stored making use of Force Modulation Microscopy (FMM) technique. FMM operated in dynamic mode and allowed simultaneous acquisition of both topographic and material-property data. It was used to detect surface elastic modulus variations on which the image analysis was performed.

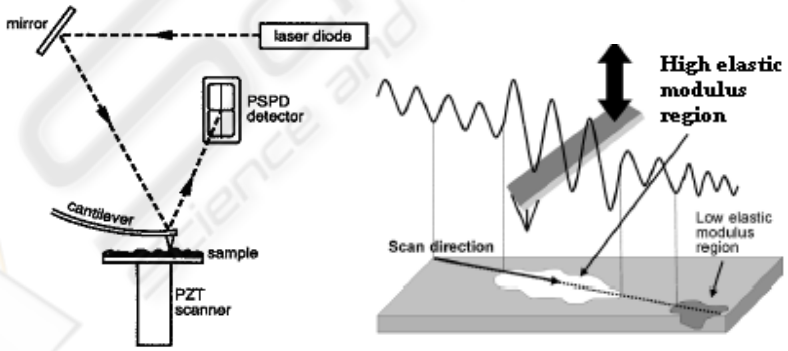

Fig. 8. On left, the schematic cartoon of an AFM. On the right, the sketch of a Force Modulation Microscope (FMM). Gradients of elasticity can be record using modulation force imaging (right) with the correspondent topography data.